METEOROLOGICAL OFFICE
EDINBURGH
14 FEB 1956
R1.
56/0039

M.R.P. 936
S.C. 111/192
18th October, 1955

Measurements of atmospheric radiation and the heat balance at the ground at Kew May, 1953 - May, 1954

by

W. T. Roach

(formerly at Kew Observatory)

AIR MINISTRY

METEOROLOGICAL RESEARCH COMMITTEE

At the time of issue this report has not been published. Any author desiring to quote this paper should refer to it as "A paper of the Meteorological Research Committee (London), M.R.P. No. 936 by Mr. W.T. Roach. A copy is available in the Library of the Meteorological Office."

M.R.P. 936
S.C.III/192
18th October, 1955

AIR MINISTRY

METEOROLOGICAL RESEARCH COMMITTEE

Measurements of atmospheric radiation and the heat balance at the ground at Kew May, 1953 - May, 1954

by
W.T. Roach (formerly at Kew Observatory)

1. Introduction

It was decided early in 1953 to use the ventilated flux radiometer advocated by Mörikofer (1951), Gier and Dunkle (1949) and others to obtain a continuous record of total net flux of radiation into the ground over a period of one year.

This project came into operation on 1st May, 1953 and continued until 12th May, 1954, during which period continuous photographic records of the following elements were obtained:-

(i) Surface temperature - measured by a fine copper-constantan thermojunction immersed in a small glass bulb containing ethylene glycol. The reference junction was maintained thermostatically at a temperature of 44.3 ± 0.1°C over the whole period.

(ii) Total net flux of radiation - measured by the ventilated flux radiometer, hereafter referred to as the VFR.

(iii) Flux of heat in soil at a depth of 6 cm. - measured by a flux plate constructed and operated on the same principle as the VFR, except that it was not sandwiched between two metal guard plates as are the elements of the VFR.

The calibration of instruments is discussed in Appendix I, and the setting up of a standard source of long-wave radiation in Appendix II.

2. Symbols

As far as possible, these follow the symbols and conventions used by Rider and Robinson (1951). We repeat the relevant symbols here.

z = Height above surface (cm.).

$T(z)$ = Temperature at height z (°K unless otherwise stated).

T_r = Radiative temperature.

$R_L(z)$ = Net vertical flux of long-wave radiation at z.

$R_s(z)$ = Net vertical flux of short-wave radiation at z.

$\downarrow,\uparrow$ = Direction of radiative fluxes through a horizontal plane.

$R_L(z)\downarrow + R_L(z)\uparrow = R_L(z)$; $R_s(z)\downarrow + R_s(z)\uparrow = R_s(z)$.

/R(z)

$R(z)$ = Total net vertical flux of radiation at height z.

= $R_L(z) + R_s(z)$.

$C(z)$ = Flux of heat by convection at height z.

$G(-z)$ = Flux of heat into ground at a depth of z cm.

$E(z)$ = Flux of water vapour at height z ($g.cm^{-2}sec^{-1}$).

$F(z)$ = Total net vertical flux of heat at z.

λ = Latent heat of evaporation of water.

$\bar{x} = \frac{1}{t}\int_0^t x\,dt$ where x is the instantaneous value of any physical quantity, and t - which may vary from 10^4 to 10^7 sec. - is defined in the context.

All fluxes of heat are in units of $mw.cm^{-2}$ unless otherwise stated.

Conventions

(i) All fluxes are considered as passing through a horizontal plane.

(ii) All fluxes are reckoned positive if directed upwards.

3. Theory

3.1. Surface temperatures

It has been shown experimentally by Robinson (1947) that T(0) - as measured by a thermometer laid directly on a short grass surface - agrees very well with $T_r(0)$ as measured by a Linke-Feussner radiometer. For instantaneous values, he found:-

$$\left|T_r(0) - T(0)\right| < \begin{cases} 3°C \text{ in conditions of strong insolation,} \\ 2°C \text{ in all other conditions.} \end{cases}$$

The standard deviations given were 1.5°C and 0.7°C respectively.

The mean value of a number of readings gave

$$\frac{1}{n}\sum_n \left[T_r(0) - T(0)\right]_n = \begin{cases} -0.5°C \pm 1.2°C \text{ in strong insolation} \\ +0.25°C \pm 0.6°C \text{ in other conditions.} \end{cases}$$

For the purposes of this investigation, therefore, it is assumed that $\overline{T_r(0)} = \overline{T(0)}$ over any period greater than an hour.

Hence we may write

$$R_L(0)\uparrow = \sigma T(0)^4 \pm 1 \text{ mw.cm}^{-2}$$

and

$$\overline{R_L(0)\uparrow} = \sigma \overline{T(0)}^4 \pm 0.2 \text{ mw.cm}^{-2} \qquad (1)$$

3.2. Ventilated flux radiometer

This measures R(z) directly. It was operated at a height of one metre above short grass, so that if R(z) is split into its components, the relevant equation is

$$R(100) = \left[R_s(100)\uparrow + R_s(100)\downarrow + R_L(100)\uparrow + R_L(100)\downarrow\right] \qquad (2)$$

/3.3.

3.3 Solar radiation

We are justified in assuming that absorption of solar radiation in the lowest metre is quite negligible, so we can write

$$R_s(100) = R_s(0)$$

Since we are interested mainly in the heat balance at the surface, it is convenient to be able to reduce the terms in eq. 2 to ground level.

$R_s(0)$ can be separated from eq. 2 and split into its components which are obtained as follows:- $R_s\downarrow$ is obtained from Kew records. $R_s\uparrow$ is the solar radiation reflected diffusely from the grass, and is not normally a routine measurement. However, one month's continuous record of this quantity was obtained during summer 1953 by M.J. Blackwell at Kew using an inverted solarimeter. His final result was

$$\overline{R_s}\uparrow = (0.25 \pm 0.01)\overline{R_s}\downarrow \text{ for short grass over one month.}$$

This figure has been adopted in the reduction of the results discussed in this paper.

Instantaneous values of the albedo of short grass can vary over quite a wide range under varying conditions, and we reproduce a table of these for interest.

Conditions	Albedo
Clear sky with high sun	0.22
Overcast sky	0.25
Low sun - altitude about 10°	0.3 - 0.4
Low sun and heavy dew on grass	$\sim$ 0.5
Overcast sky and heavy rain	0.1 - 0.2

In general, the heavier the rain, the lower the albedo, but whether this is a real or instrumental effect has apparently not been tested.

3.4. Long-wave radiation

$$R_L(100) = R_L(0) + \int_0^{100} \frac{\partial R_L(z)}{\partial z}\, dz \qquad (3)$$

The integral term usually assumes an appreciable value under clear skies - especially under a hot sun, when it may be of the order of 1 mw.cm^{-2} for short periods. When averaged over a day or more, it becomes negligible. Hence we assume

$$\overline{R_L(100)} = \overline{R_L(0)}$$

and

$$\overline{R_L(100)}\uparrow = \overline{R_L(0)}\uparrow = \sigma\,\overline{T(0)}^4 \qquad (4)$$

It follows from this and 3.3 that

$$\overline{R(100)} = \overline{R(0)}$$

From the foregoing, eq. 2 can be rewritten

$$\overline{R(0)} = 0.75\,\overline{R_s}\downarrow + \overline{R_L}\downarrow + \sigma\,\overline{T(0)}^4 \qquad (5)$$

This is the equation used in reducing the results, and represents the radiative heat balance at the ground.

/3.5.

3.5. Earth flux plate

This gives a measure of the heat flow by conduction through the soil at a depth of 6 cm. The equation of heat conduction is

$$G(-z) = k_s(-z)\left(\frac{\partial T}{\partial z}\right)_z \equiv \alpha V \qquad (6)$$

where k_s = thermal conductivity of soil ($mw.cm^{-1}\ deg^{-1}$)

α = calibration constant of the flux plate ($mw.cm^{-2}/\mu V$ output)

V = output from flux plate in μV.

It has been found that α has a slight dependence on the ratio of k_s to the thermal conductivity of the material of the flux plate former - in this case paxolin. Experimental work shows that an increase in k_s of 40 to 1 results in an increase in α of only 1.6 to 1. This may be expressed as an approximate power law $\alpha \propto k_s^{1/8}$. Since k_s varies by a factor of about 3 over the year, α varies less than 10% on either side of a mean value.

3.6. Energy balance equation

We can now write down the equation for the energy balance in the top 6 cm. of soil. First we have the expression for flux of heat across the surface.

$$F(0) = C(0) + \lambda E(0) + R(0) = G(0)$$

since energy flow across the surface is continuous. The divergence of heat energy in the layer considered is

$$F(0) - F(-6) = C(0) + \lambda E(0) + R(0) - G(-6) \qquad (7)$$

on the assumption that flow of heat in the soil is practically all conductive; i.e., that transfer of heat by processes involving the movement of water or water vapour is negligible.

Over a period of one year, we can write

$$\overline{F(0)} - \overline{F(-6)} = 0,$$

and even after a few days

$$\left|\overline{F(0)} - \overline{F(-6)}\right| \ll \left|\overline{C(0)} + \lambda\overline{E(0)} + \overline{R(0)}\right|$$

Hence we can write eq.7

$$-\left[\overline{R(0)} - \overline{G(-6)}\right] = \overline{C(0)} + \lambda\overline{E(0)} \qquad (8)$$

The L.H.S. of eq.8 consists of measurable terms, and if $\lambda\overline{E(0)}$ can be estimated from evaporation tank readings or by other methods (Penman (1950)), a value for $\overline{C(0)}$ can be obtained.

Finally, we should expect that over a period of one year

$$\overline{G(-6)} = 0. \qquad (9)$$

So that over this period, eq.8 becomes

$$-\overline{R(0)} = \overline{C(0)} + \lambda\overline{E(0)} \qquad (10)$$

/4.

4. Discussion of records

4.1. Reduction of records

There is available a complete year's record of surface temperature, and so $R_L(0)\uparrow$, and flux of heat into the soil, $G(-6)$. Hourly means have been tabulated for about the first six months and daily means for the whole year.

With total radiation, $R(0)$, a difficulty arises. Tests by the N.P.L. on the paint used to blacken the surfaces of the VFR showed that while the paint had a very high absorptivity (0.98 for radiation from a black body source at 473°K), it was rather susceptible to damage - the mattness of the paint surface is easily ruined. Hence for most of the year, it was the practice to cover the radiometer plates whenever rain occurred or was forecast, so that half the total possible record of $R(0)$ was lost.

The main difficulty arises from the fact that the recorded half of $R(0)$ will not be representative of the unrecorded half, and if it is desired to extract monthly or even daily means of $R(0)$, some method has to be found of estimating R over the blank periods. Returning to eq.5, we see that, since continuous records of $R_S\downarrow$ and $T(0)$ are available, the problem reduces itself to estimating $R_L\downarrow$ in order to obtain R.

4.1.1. Estimation of $R_L\downarrow$

There now exists a large amount of literature on the estimation of $R_L\downarrow$ by empirical formulae and by radiation charts; the formulae involving surface parameters only, and the charts taking some account of the vertical distribution of temperature and humidity in the lower troposphere. The latter method, if practicable, is to be preferred, since it is based on the equation of radiative transfer and experimental results.

The normal procedure in drawing a radiation chart for a given situation is to obtain vertical soundings of temperature, pressure and dew-point from the relevant Daily Aerological Record. From these data, a profile of temperature against precipitable water vapour is obtained, and hence, using experimental data, of $\sigma T(p)^4$ against emissivity of the column of precipitable water vapour between the ground and height corresponding to pressure p. In practice, this would be an impossibly laborious process for our purposes, so that drastic cuts had to be made in the programme of work.

The procedure adopted was to draw curves on the Kew Radiation Chart representing the humidity-temperature profiles in an atmosphere having a lapse rate of 6.5°C/Km. for five different values of screen temperature over a range of about 273°K to 300°K. For each screen temperature two curves were drawn, one for a saturated atmosphere, and one for a relative humidity throughout of 50%; ten curves in all.

It was then found sufficiently accurate to draw any actual curve from a D.A.R. sounding using the arbitrary curves as guidance, and making allowance for conditions of inversion or steep lapse near the ground.

4.1.2. Cloud cover

The radiation chart can only take account of a completely clear sky, or a completely overcast sky if the height and temperature of the cloud base are known - the latter then being considered to radiate as a black body at cloud base temperature.

For intermediate cloud cover, we have adopted the following intuitive expression:-

$$\overline{R_L(c)\downarrow} = c\overline{R_L(1)\downarrow} + \overline{(1-c)R_L(0)\downarrow} \qquad (11)$$

/where

where c is the fraction of sky covered (the bracketed quantity after $R_L\downarrow$ represents cloud amount and not height for this short section only). Eq.11 is similar to, but less restricted than Ångström's expression, which, using the notation above, is

$$R_L(c) = (1 - 0.9c)R_L(0)$$

The constant 0.9 restricts the use of the expression to rather low cloud bases.

Neither expression is valid for instantaneous values of $R_L\downarrow$ or R_L, since c as measured by climatological stations is represented by an expression of the form

$$c = \frac{1}{2\pi}\int_{cloud} d\Omega$$

where $d\Omega$ is an element of the total solid angle of sky obscured by cloud. From the point of view of radiation, however, an expression of the form

$$c_r = \frac{1}{\pi}\int_{cloud} \cos\theta . d\Omega$$

is relevant, and it follows that R_L is strongly dependent on cloud distribution as can soon be seen on working out one or two arbitrary examples. Over a period of an hour or more, however, the effects of distribution would be expected to average out and become negligible, so that we assume that $\bar{c} = \overline{c_r}$, and eq.11 is probably as reasonable as can be expected. It has been found practically impossible to check eq.11 against actual records. Cloud amount observations given in the Daily Weather Report are instantaneous values tabulated every six hours, and these readings, coupled with a survey of the general weather conditions prevailing, form the only direct method of obtaining $\bar{c}$, and any comparison of the observed value of $\overline{R_L\downarrow}$ over this period with the value of $\overline{R_L\downarrow}$ obtained by substituting the relevant value of $\bar{c}$ in eq.11 will certainly not be any more reliable than the direct use of this equation.

Indirect estimates of $\bar{c}$ can be obtained from sunshine records and night sky camera records. For instance, the quantity $(1-\bar{c})$ will be roughly correlated to the ratio of actual to total possible hours of sunshine, but the correlation depends upon time of year, altitude of sun, and type of cloud to name but a few variables. A comparison of the quantity $(1-\bar{c})$ - which we shall call A - and actual/total possible number of hours of sunshine - which we shall call B - was made for the months June and December 1953, and the values of A/B were about $\frac{3}{4}$ and 1.6 respectively. The values of A/B for individual days showed a wild scatter over a range of as much as 3 to 1, and it appears that this method of estimating $\bar{c}$ is of not much use over periods less than a month.

Cloud amount estimation at night is more difficult and therefore less reliable; in any case, these observations are not made at Kew between 2100 and 0600, so that no comparison with night sky camera records is possible.

4.2. Summary of results and comparison with estimates

Table I summarises the monthly and annual means of the various quantities contributing to the heat balance, and Fig.1 (a) and (b) illustrates the annual variation of the more important terms. Table II summarises the readings of the surface thermometer, which are thought to have some climatological interest.

4.2.1. Surface temperatures (Table II)

The quantitative and qualitative variations of surface temperature on short grass throughout the year were much as expected in all types of

weather. In particular, the marked discontinuity of rate of temperature change about dusk under clear skies reported by several observers was never observed at Kew.

As expected, the monthly and annual mean temperatures are not appreciably different from the monthly and annual mean screen temperatures. The diurnal range is just about twice that of screen temperature all the year round. In summer, diurnal ranges of 30°C were not uncommon, and although the greatest range recorded was 31.2°C it is considered that ranges up to 40°C are quite possible - especially in periods of summer drought - and would be most likely to occur between about mid-May and mid-June. Extreme values for the year were 312°K and 261°K. Probable absolute extremes at Kew are 320°K (325°K over parched brown turf) and 255°K.

The mean times of occurrence of daily maxima and minima are substantially earlier than those of screen temperature: the maxima are about $2\frac{1}{2}$ hr. earlier in summer and 1 hr. in winter, while the minima are about $1\frac{1}{2}$ hr. earlier in summer and 2 hr. in winter.

4.2.2. Total radiation

The monthly value of $\overline{R(0)}$ varies from about -10 mw.cm^{-2} in midsummer to about +1 mw.cm^{-2} in midwinter, so that the ground becomes a heat sink by radiation from about mid-November to mid-February. (See Table I).

The annual mean of -4.0 mw.cm^{-2} is probably numerically a little below normal due mainly to rather poor summer weather when increased cloudiness has the greatest effect on incoming solar radiation.

Extreme values of R(0) numerically exceeding -80 mw.cm^{-2} occurred during June and July, and a peak value of -91 mw.cm^{-2} was recorded soon after midday on 20th June. From eq.5, we find that $R_S\downarrow$ simultaneously reached an extreme value of -135 mw.cm^{-2}, which compares with the Solar Constant (-138 mw.cm^{-2}). This was a day of brilliant sunshine, with large Cu and Cb typical of a polar maritime air mass in summer. This record has been reproduced in the series of charts included as specimens later in this paper.

Considering the probable error of R(0) we see from eq.5 that the main uncertainty arises from errors in $\overline{R_L\downarrow}$. While it may be as large as ±2 mw.cm^{-2} if estimated for a few hours, it is thought that it is not likely to exceed ±0.5 mw.cm^{-2} over a month, and we feel fairly safe in quoting the mean for the year with this error. It is noted that there will be an error of estimation for the unrecorded half of $\overline{R(0)}$ - and therefore of $\overline{R_L\downarrow}$ - and instrumental errors for the recorded half which are not likely to be substantially less than the first type. Furthermore, the value of $\overline{R_L\downarrow}$ over a month is found to lie for most of the time within a range of 5 mw.cm^{-2}, which automatically sets limits to the magnitude of possible errors.

4.2.3. Long-wave radiation

The mean value of $\overline{R_L}$ for the year was 3.8 mw.cm^{-2}. This is substantially less than one is led to expect from estimates based on empirical and scanty observational data found scattered in the literature. The discrepancy may be partly due to the presence of thin layers of tenuous high cloud which is now known to be present in much greater quantity than was thought until recently; it may also be due to the imperfections inherent in the construction of radiation charts. Robinson (1947) found that there was nearly always an additional downward component of long-wave radiation when observations were compared with estimates given by radiation charts. There were about half-a-dozen occasions when good agreement was obtained - occasions of "minimum radiation" as called by Robinson - which suggests that these were rare occasions when the sky was exceptionally clear and free from high cloud.

The presence of this cloud was borne in mind when estimating $\overline{R_L\downarrow}$ as described earlier, and it was noticed that a good indication of its presence was given by the difference between screen and ground temperatures. On a clear night, this can reach 5°C (and more over snow), but was more often 2-3°C. On a hot day in June, the difference is usually around 10°C, but may reach 15°C.

R_L can vary from zero, or even slightly negative (-0.2 mw.cm^{-2}) to about +10 mw.cm^{-2} on clear nights before the development of a large inversion near the ground, and to upwards of +15 mw.cm^{-2} on very hot days - especially in May and June.

$R_L\downarrow$ averaged about -33 mw.cm^{-2} over the year, and ranged between extreme values of -41 mw.cm^{-2} during the heat-wave of the first week in August to -21.5 mw.cm^{-2} during the very severe spell of easterly winds early in 1954.

4.2.4. Earth flux plate

The numerical magnitudes of the fluxes involved here are an order of magnitude less than those associated with R(0). The monthly values of $\overline{G(-6)}$ varied from about -0.6 mw.cm^{-2} in May to about +0.6 mw.cm^{-2} in January. Normally, one expects the phase of the curve of ground heat flow to lead that of air temperature by about 90°, but the extreme of heat flow occurring in January - about 2 months late - is due to the exceptional mildness of November and December 1953.

$\overline{G(-6)}$ over the year was expected to be practically zero. In fact, it came to +0.05 mw.cm^{-2} which corresponds to a total heat loss by the ground below 6 cm. of 350 cal.cm^{-2}yr^{-1}. Now the temperatures at depths of 1 ft. and 4 ft. increased between May 1953 and May 1954 by 0.4°C and 0.3°C respectively, which corresponds to a flux of the order -50 cal.cm^{-2}yr^{-1}. These figures are to be compared with a total change of heat content of the ground of the order 2000 cal.cm^{-2} between winter and summer. These results made the reliability of the flux plate records suspect, and when the flux plate was unearthed in July 1954, it was found to have sunk 2 cm. and to have acquired a tilt of about 15° to the horizontal. The discrepancy may however be a measure of the extent to which heat is transferred through the 6 cm. level by processes involving the evaporation and condensation of water within the soil, though this suggestion implies the downward movement of water vapour. Rough calculation shows that it is much too large to be explained by mass movement of liquid water. While little significance can be attached to the annual mean, this is in any case very small compared to the other fluxes considered, and the discrepancy does not invalidate the records as a means of estimating $\overline{G(-6)}$ over shorter periods. Values of G(-6) are not likely to be in error anywhere by more than 20%.

As expected, there is a high correlation between the diurnal range of temperature at the ground and heat flux at -6 cm. (0.89 for May 1953) but with an annual variation in their ratio. This ratio decreased from 0.29 mw.cm^{-2}/°C in May 1953 to about 0.18 in January 1954, and had risen again to 0.25 by April 1954. Heat conduction in the soil is dependent on thermal diffusivity $k_s/\rho c$. The thermal capacity, ρc, is 2 to 3 times greater in winter than in summer due to much greater average moisture content, so that changes in heat flow in the soil will respond less to changes in surface temperature, whereas there is an increase in k_s in winter which partly offsets this effect, and the net result is an increase in the above-mentioned ratio of about 1.6 to 1 from winter to summer, with maxima and minima in May and November.

4.2.5. Heat balance

We refer back to eq.8,

$$-\left[\overline{R(0)} - \overline{G(-6)}\right] = \overline{C(0)} + \lambda\,\overline{E(0)}$$

/The

The work of Penman (1950) and others on evaporation estimation enables us to obtain a fairly reliable estimate of monthly means of $\overline{\lambda E(0)}$ using the available records at Kew.

Penman derives an expression for the rate of evaporation, E_o, from an open water surface in terms of net radiation, mean vapour pressure, temperature, and wind speed at 2 m. He converts the energy terms to evaporation equivalents (1 mw.cm^{-2} day $\equiv$ 0.35 mm.day^{-1}) and the final value of E_o is multiplied by an empirical factor f to allow for the surface under consideration. For short, moist turf, he finds that f varies from about 0.6 in winter to 0.8 in summer.

Since records of R(0) are available, the monthly values were substituted straight into Penman's expression, and the final value of E_o compared with the measured value given by the Kew evaporation tank. Finally, values of fE_o - i.e. $\overline{\lambda E(0)}$ - were tabulated (both the measured and calculated values), and monthly values of $\overline{C(0)}$ thus obtained. (See Table I). It was found that the Kew evaporimeter read lower in summer and higher in winter than the estimates. The value of $\overline{\lambda E(0)}$ for the year was +4.2 mw.cm^{-2} from Penman's formula and +3.6 mw.cm^{-2} from the tank record. The rainfall for the period (P) was 513 mm., the corresponding rate of supply of energy ($\overline{\lambda P}$) being roughly 4.0 mw.cm^{-2}. Since it is difficult to visualize a year with a negative run-off of rainfall, the tank figure (when corrected by the factor f) is almost certainly the more reliable. Even then, a run-off amounting to only 10% of the rainfall seems too small. The year 1953 was notably dry, and it might be expected that there must have been periods when the turf was affected by drought, and hence modification of the factor f necessary. However, most of the deficit occurred in the winter months, and at no time did the grass appear other than bright green.

This method of estimation only gives us monthly means of $\overline{C(0)}$ which show a small annual variation with an amplitude and an annual mean of the same order of magnitude as the probable error.

4.3. Specimens of photographic records

These are reproduced in chronological order at the end of this paper. We confine ourselves to brief comments on each of them here.

a. 4 June 1953

A day of brilliant sunshine, cold NNE winds and large cumulus typical of a polar maritime air mass in early summer. The air is very dry - relative humidity less than 50% - and fluctuations of surface temperature are enormous - approaching 20°C.

b. 9 June 1953

A rare example of a perfect summer day. The sky was perfectly clear for at least 24 hours apart from small, scattered cumulus in the afternoon. The temperature was not too high - max. 69°F (294°K) at Kew. The synoptic charts show that S. and E. districts of England were situated in a col on this day.

c. 20 June 1953

It is interesting to compare the trace of R(0) with that in chart b. In 20 June, large white cumulus enormously increase the diffuse component of solar radiation reaching the VFR, and, in sunny intervals, give a resultant R(0) at times not far short of twice that recorded on a perfectly clear day at the same time of year.

d. 16-17 November 1953

The main feature of interest here is the sudden arrival of fog at about 0110 on the 17th. When fog forms in situ, the net flux of radiation (at night)

/gradually

gradually approaches zero over a period of 2 or 3 hours. Here, the fog has already formed, and is drifting about. An occlusion from a deep depression was lying almost stationary ENE-WSW across N. England, with widespread fog developing in S. districts.

e. 29-30 November 1953

This shows the effect of the arrival of a warm sector on earth flux at a depth of 6 cm., and the levelling out of T(0) as the sky clouds over.

f. 27-28 January 1954

A day during, and typical of, the severe easterly spell persisting at this time.

Surface temperature rose just above 273°K for about an hour in the early afternoon, and dropped to about 263°K at night. The day was mainly cloudy - $\frac{5}{8}$ to $\frac{7}{8}$ of Sc - decreasing to small amounts at night. The top layer of soil is already frozen, but not yet to the depth of the flux plate. Note how the fluctuations of G(-6) have been ironed out. This is the subject of a short note later in this paper.

g. 7 February 1954

Note the effect on G(-6) of the commencement of the thaw.

h. 15 February 1954

An example of an exceptionally dull, murky day, with very heavy cloud and intermittent drizzle. At this time, Kew was in the vicinity of a slow moving occlusion marking the boundary of the cold continental air experienced recently. On this occasion, it did not reach us.

j. 31 March 1954

This short record indicates what happens to the record of R(0) when rain does get on the top surface of the radiometer plate. This was a day of heavy showers and bright intervals. Rapid evaporation of rain from the top surface of the VFR by its blower causes the wet bulb effect shown. This shower was the first of several, culminating in a thunderstorm about 1700.

4.4. The effect of freezing in the soil upon G(-6)

When the moisture in the soil begins to freeze, the temperature of the layer in process of freezing at any given time will be locked at 0°C for some time while its latent heat is being conducted away through the already frozen layer above. The presence of this freezing layer has the effect of stabilising the temperature profile beneath it, i.e., fluctuations in T(0) have no effect on the temperature gradient below the freezing level, and hence upon the heat flow. The latter does decrease very slowly as heat is drained from the lower layers, and the gradient slackens somewhat. For instance, at Kew during the last week of January, the temperature at 6 cm. remained very near 0°C all the time, while the temperature decreased from about 4°C to 3°C at 1 ft., causing G(-6) to decrease in proportion.

When the freezing level reaches and passes below the level of the flux plate, G(-6) resumes its normal variations in sympathy with T(0) until the thaw sets in. When this occurs, the temperature of the whole of the frozen layer rises to melting point, and remains there for a day or two, during which time the flux plate (being enclosed in an isothermal layer) records zero net flux of heat.

/All

All this sequence of events in fact occurred between 24th January and 7th February 1954. Freezing commenced on the 24th, and after just thawing out under the midday sun on the 25th, continued until the 6th February. Freezing reached the flux plate depth after a week, and eventually extended to about 10 cm. depth.

4.5. Conclusion

The emphasis of this paper has been on the presentation of results of measurements of some meteorological elements not hitherto recorded continuously over a comparable period of time, and preliminary interpretation has shown the results to be, in the mean, much as expected.

The only previous work of this nature that we could find is due to Falckenberg and Bolz (1950), who made ½ to 1 hourly measurements of $R_L\downarrow$ and $R_S\downarrow$ - the latter being the sum of the direct and diffuse components of solar radiation as measured by them - over the period 1.4.1947 to 31.3.1948 using a vibration pyranometer, which employs the same principle as the VFR. These measurements were made in Lat. 54°11'N., Long. 12°5'E., and they obtained a value for $\overline{R_L\downarrow}$ for the year of -32 mw.cm^{-2}. Their results were expressed as mean values every ten days, and these ranged from -26 to -38 mw.cm^{-2} for $\overline{R_L\downarrow}$ during the year.

The main use of records of total radiation has been so far simply to provide direct measurements of a major term in the heat balance equation for the surface. If these records are to be used to interpret more transient phenomena in the atmosphere - and especially near the surface - they need to be supplemented by continuous records of many more elements than surface temperature and earth flux. Furthermore, it seems that little further information about radiative processes in the atmosphere can be obtained by measurements of total fluxes of atmospheric radiation near the surface unless these are supplemented by spectral analysis of the long-wave radiation.

Acknowledgments

I should like to express my indebtedness to Dr. G. D. Robinson and Mr. M. J. Blackwell for many useful discussions and help during this work, and to Mr. J. Gordon and Mr. A.J. Lander who installed the apparatus on site and made the initial measurements.

REFERENCES

Deacon, E.L.	1950	Q.J.R. Met. Soc., 76, 479.
Falckenberg, G. and Bolz, H.M.	1950	Zeit. Met. 4, 65.
Hatfield, H.S. and Wilkins, F.J.	1950	J. Sci. Inst., 27, 1.
Gier, J.T. et al.	1949	University of California, Thermal Radiation Project Report.
MacDowall, J.	1954	Meteorological Research Papers, Air Ministry, London, No. 858.
Mörikofer, W.	1951	Proc. of U.G.G.I., Brussels, Compte rendu du Symposium sur le Rayonnement, 207.
Penman, H.L.	1950	Q.J.R. Met. Soc., 76, 372.
Robinson, G.D.	1947 1950	Ibid., 73, 127. Ibid., 76, 479.
Goody, R.M. Robinson, G.D.	1951	Ibid., 77, 151.
Rider, N.E. Robinson, G.D.	1951	Ibid., 77, 375.

APPENDIX I

Calibration of instruments

1. Surface temperature

It is probably sufficiently accurate to use tables of thermo-emfs for copper-constantan junctions in order to convert the galvanometer deflections into temperatures, but the calibration was checked by a conventional method.

2. Earth flux plate

The method used at Kew was that advocated by Hatfield and Wilkins (1950), and need not be discussed here.

3. Ventilated flux radiometer

Four methods of calibration - two in the laboratory and two on site - have been described by MacDowall (1954).

Briefly, these were:-

(i) Comparison of outputs of VFR and Ångström pyrheliometer using a voltage-controlled 2 Kw. tungsten lamp.

(ii) Exposure of one side of radiometer plate to a black body source through an aperture of known size.

(iii) Comparison of direct reading of R(0) on site with value of R(0) obtained by measuring $R_S\uparrow$ and $R_S\downarrow$ with solarimeters, and $R_L\uparrow$ and $R_L\downarrow$ with the surface thermometer and Linke-Feussner radiometer.

(iv) Direct side-by-side comparison on site of outputs of a laboratory calibrated VFR and the VFR on site.

The continuously recording radiometers on site could not be calibrated in the laboratory directly because the ventilation supply was a permanent fixture on site, and could not be transferred to the laboratory.

It was found that (i) provided the most manageable and reliable method of calibration, so that we shall discuss it in some more detail with emphasis on precautions and possible sources of error.

3.1. Short-wave calibration of VFR

Comparison is made between outputs of the Ångström pyrheliometer or the calibrated Linke-Feussner radiometer - which are directional radiometers, their solid angle of acceptance being of the order 0.05 steradians - and the VFR, which receives radiation from a hemisphere on each side and records the difference.

Hence the main problem is to account for all stray sources of long-and short-wave radiation not "seen" by the directional instruments, but which contribute to the output of the VFR.

3.1.1. Extraneous sources of short-wave radiation

These include light from unmasked windows, other lights in the laboratory, reflections from walls of light from the tungsten lamp escaping round the sides of the VFR.

In practice, the laboratory is blacked out for this calibration, but enough light to see what one is doing with comfort is permissible. It must be

/remembered

remembered that the human eye's response to light is logarithmic, whereas the radiometer response is linear, and it requires a surprising amount of light to affect the readings by as much as 1%. For example, imagine replacing the 2 Kw. lamp by a 20 watt bulb.

3.1.2. Extraneous sources of long-wave radiation

These are far more troublesome. They are:-

(i) Emission from heated lamp housing. This is remedied by the interposition of a sheet of glass which is opaque to wavelengths beyond about 3 μ. The placing of a second sheet behind the radiometer thus completes a fairly effective shield to all long-wave radiation.

(ii) The heat given out by the tungsten lamp is dissipated with the help of a blower with the result that a vigorous column of hot air rises to the ceiling where it spreads out and steadily warms the ceiling, providing a steadily increasing source of long-wave radiation of which an appreciable part can pass over the top of glass sheets direct to the radiometer plates. During normal calibrations, the angle of incidence of this radiation is not less than 60°, and the effect is small, but becomes very appreciable when cosine law tests are made by rotating the radiometer about a horizontal axis, and may amount to 15% of the total flux if a third glass sheet is not placed above the VFR.

(iii) The sheet of glass between the radiometer and source will be absorbing much more long-wave radiation than the sheet behind the radiometer, and will heat up after a few minutes' exposure to a hot lamp, thus causing a steady drift output from the radiometer, and since these sheets occupy 0.8 to 0.9 of the radiometer's field of view, a temperature difference of 1°K between the sheets is sufficient to cause a drift of some 5% in output. Hence careful and frequent zeroing by screening the lamp is necessary. In practice, it was found necessary to zero before and after each reading.

The only criticism of this method as a complete one is that we employ a short-wave source in the calibration of an instrument that is primarily intended to measure both short- and long-wave radiation. We use, as our basis for justification, the results of the N.P.L. tests on the absorptivity of the paint used to coat the radiometer surfaces. They found this to vary by less than 1% from 0.98 for radiation from black-body sources ranging from 2850°K to 470°K.

We conclude that providing the comparison sub-standard radiometer is well calibrated, it should be possible to rely on a VFR calibration to $\pm$1%; certainly within $\pm$2%.

3.2. Performance and applications of the VFR

It has already been noted that the radiometer is well suited to field work. It works much better and more reliably than is usually expected at first sight. It is robust, easily made portable, and is simple and inexpensive to build. It should give instantaneous values of R under most conditions to $\pm$ 5%, providing it is calibrated carefully and reasonably often, and repainted when the surfaces show signs of marked deterioration.

As a result of weathering tests made in April 1954, it was decided that the radiometer can be left exposed at all times, provided allowance be made for the decrease of absorptivity which becomes more important in the visible wavelengths - especially at large angles of incidence. This is most important for direct radiation coming from a low sun.

Rain has little harmful effect, and, in fact, serves to wash the top surface free of the grey dust deposit which otherwise appears to form -

/probably

probably due to inadequate filtering of the blast of air. Unfortunately, if one attempts to introduce finer filters, the speed of the air blast is inevitably reduced.

In routine use, it is recommended that the radiometer be reversed to ensure washing of both sides, or better, that the under surface be sprayed with water when it appears necessary.

3.2.1. Corrections to records of R(0) for prevailing wind-speed.

The effect on the calibration constant of the VFR of wind of various speeds and directions relative to the orientation of the VFR on site was investigated thoroughly by MacDowall (1954), who found that for wind-speeds less than about 20 mph the change in calibration never amounted to more than ±2% for any wind direction. At the level of the radiometer on site, the wind-speed rarely reached this value, and the mean wind-speed at this level at Kew is probably of the order 2-3 mph throughout the year. The correction for this speed is quite negligible, and no attempt has been made to correct the monthly values of $\overline{R(0)}$ for wind-speed.

APPENDIX II

A standard source of long-wave radiation

It is proposed to discuss the setting up of a black body cavity radiator as the ultimate standard of long-wave radiation at Kew, concluding with a brief reference to the long-wave calibration of the Linke-Feussner radiometer against the black body. This sets up the Linke-Feussner radiometer as a substandard for calibration of other types of radiometer, or for directional observations of atmospheric radiation.

One of the main reasons for including this section in this paper is because there seems a tendency among workers in this field to refer to calibration of their radiometers against black bodies with little or no mention of the precautions and corrections necessary in such measurements beyond the usual statement that the radiation emerging from the cavity is black-body emission to better than 99% at the temperature of the black body with no mention of how this temperature is measured.

The black body cavity radiator in use at Kew until recently was constructed by Dines in 1920, and had the following main disadvantages:-

(i) Inadequate stirring of water in jacket

(ii) No internal source of heating in water jacket

(iii) No temperature control

(iv) No provision for measuring temperature differences between the cavity walls and the water jacket

(v) Inadequate lagging - partly a function of age

(vi) No convenient form of mounting.

A new black body cavity radiator was designed and built at Kew this year in which these disadvantages have been eliminated as follows:-

(i) Efficient stirring is achieved by a pump which draws water from the bottom of the water jacket into two vertical channels which throw the water out at the top. The rate of pumping is of the order of 30 litres min^{-1}, so that the entire volume of water is pumped through in less than a minute. Circulation of the water is promoted by the shape of the cavity, which is an upright cone instead of the inverted cone used in the Dines' black body (see Fig. 2).

(ii) Internal heating is achieved with a 2 Kw. immersion heater which heats the water from 10° to 50°C in about 30 minutes.

(iii) Temperature control at any desired temperature is obtained by passing enough current through the heater to balance the small loss of heat by cooling. This amounts to about 30 watts for a temperature difference of about 30°C between room and water jacket.

Temperature is read by an N.P.L. calibrated thermometer, and it is possible to keep this constant at any desired value, with supervision, to within ±0.01°C over any desired period; this is scarcely possible by any other method.

The rate of supply of heat caused by the viscous dissipation of the kinetic energy imparted to the water by the pump appears to be of the order of 10 watts, which decreases as the temperature increases. The pump motor is rated at 80 watts.

(iv) For accurate work, it is necessary to know the temperature field within the cavity, and the difference between the temperatures of the water and the

/cavity

cavity walls. This has been achieved by installing suitably placed thermojunctions in the cavity; they can be compared in turn with a reference thermojunction placed adjacent to the thermometer bulb in the water jacket. A floating junction is also provided as a probe; it can also be immersed in a Dewar flask of ice if it is desired to cross-check temperature readings of the reference junction with the thermometer.

(v) The jacket is surrounded by a thick layer of felt and cotton wool, and the whole contained in a wooden box. The efficiency of the lagging is nearly an order of magnitude better than the Dines' black body.

(vi) The black body is mounted with its cavity looking vertically downwards, but with enough space to insert the Linke-Feussner radiometer below looking vertically up into it.

Cardboard masks are provided to limit the aperture of the black body if desired, and an outlet is provided for the water in the jacket in case it is desired to drop the temperature quickly by replacing some of the hot water by cold.

With careful work, it should be possible to obtain the radiation temperature of the cavity walls reliable to within $\pm 0.05°C$ - i.e. σT^4 to about ± 0.03 mw.cm^{-2}, which is about 1 part in 1000. However, σ itself is not known to this degree of accuracy.

Disadvantages of the new black body

(i) Excessive weight - well over 1 cwt. when water jacket is full. This does not matter unless it becomes inconvenient to have the black body in one position permanently.

(ii) Rather small temperature range - room temperature up to 50°C, although it could be adapted to work up to 100°C.

(iii) No cooling system. Since radiometers looking at the sky are generally losing energy to it, it would be useful if a cold black body were available.

(iv) The water jacket does not extend down to level of aperture, which requires that the temperature field within the aperture be measured carefully.

Calibration of the Linke-Feussner radiometer

This has been described by Robinson (1947), but the following remarks refer to precautions taken and corrections made in a recent calibration.

The Linke-Feussner thermometer - which measures the temperature of the thermopile - was calibrated against an N.P.L. calibrated thermometer in a stirred water bath. Correction was made for stem exposure of the latter; the former was completely immersed as its stem and bulb are practically at a uniform temperature in use.

The output of the Linke-Feussner is of the order 10 μV for a temperature difference of about 20°K between the black body and the thermopile of the Linke-Feussner, so that stray thermo-emfs can be a source of trouble if not accounted for by suitably placed copper reversing switches in the output circuit.

Measurement of the temperature profile between the Linke-Feussner thermopile and the cavity walls was made, and the humidity measured with an Assmann psychrometer, and the correction for absorption of radiation by water vapour and CO_2 computed by constructing a radiation chart. The final calibration obtained was estimated to be reliable to about $\pm$ 1%.

Table I

Summary of Results

MONTH	$\overline{R(0)}$	$\overline{R_s(0)}$	$\overline{R_L(0)}$	$\overline{\sigma T(0)^4}$	$\overline{R_L(0)\downarrow}$	$\overline{G(-6)}$	$\overline{-(R-G)}$	$\overline{\lambda E(0)}$ calc.	$\overline{\lambda E(0)}$ Kew Tank	P	$\overline{\lambda P}$	$\overline{C(0)}$ calc.	$\overline{C(0)}$ Tank	$\overline{h}$
1953														
MAY	-8.6	-14.4	+5.8	+39.2	-33.4	-0.6	+8.0	+8.6	+7.1	39.5	3.7	-0.6	+0.9	11.7
JUN.	-8.4	-12.9	+4.5	+39.9	-35.4	-0.4	+8.0	+7.9	+6.6	46.6	4.4	+0.1	+1.4	11.9
JUL.	-9.6	-14.1	+4.5	+40.4	-35.9	-0.1	+9.5	+9.2	+6.8	91.8	8.6	+0.3	+2.7	8.8
AUG.	-9.0	-13.0	+4.0	+40.8	-36.8	-0.2	+8.8	+8.3	+7.0	43.9	4.1	+0.5	+1.8	14.6
SEP.	-5.5	-9.7	+4.2	+38.7	-34.5	+0.2	+5.7	+5.0	+4.3	50.9	4.8	+0.7	+1.4	13.3
OCT.	-1.6	-4.2	+2.6	+36.7	-34.1	+0.4	+2.0	+1.6	+1.6	58.2	5.5	+0.4	+0.4	12.5
NOV.	+0.2	-2.1	+2.3	+35.7	-33.4	+0.3	+0.2	+0.6	+0.8	37.6	3.5	-0.4	-0.6	12.1
DEC.	+0.7	-1.2	+1.9	+34.8	-32.9	+0.4	-0.3	+0.2	+0.7	12.8	1.2	-0.5	-1.0	10.1
1954														
JAN.	+1.3	-2.0	+3.3	+32.6	-29.3	+0.6	-0.7	+0.8	+0.7	23.4	2.2	-1.5	-1.4	12.3
FEB.	-0.3	-3.0	+2.7	+33.0	-30.3	+0.2	+0.5	+1.2	+1.3	49.6	4.7	-0.7	-0.8	7.9
MAR.	-2.5	-5.7	+3.2	+34.9	-31.7	0.0	+2.5	+2.4	+1.8	49.0	4.6	+0.1	+0.7	11.4
APR.	-4.9	-10.7	+5.8	+35.8	-30.0	-0.1	+4.8	+4.4	+4.2	9.7	0.9	+0.4	+0.6	20.0
YEAR	-4.0	-7.8	+3.8	+36.9	-33.2	+0.05	+4.1	+4.2	+3.6	513.0	4.0	-0.1	+0.5	12.2
P.E. ±	0.5	0.2	0.5	0.2	0.5	0.1	0.5	0.3	-	-	-	1.0	1.0	-

All units are in mw.cm^{-2} except for h which represents the mean number of hours per day that the radiometer was recording, and P, which denotes monthly rainfall in mm. $\overline{\lambda P}$ is the evaporation equivalent.

\+ denotes flux or net flux directed upwards.
\- " " " " " " downwards.

Table II

Surface Temperature: degrees Kelvin

MONTH 1953	Mean Max.	Mean Min.	Abs. Max.	Abs. Min.	Mean Diurnal Range	Abs. Range	Lowest Max.	Highest Min.	Max. Diurnal Range	Min. Diurnal Range	Time of Diurnal Max.	Time of Diurnal Min.
MAY	299.2	279.7	311.2	271.7	19.5	39.5	283.5	287.8	30.2	3.7	1251	0229
JUN.	301.5	282.0	309.2	276.3	19.5	32.9	288.0	288.9	27.1	7.4	1247	0217
JUL.	302.5	283.2	311.7	279.8	19.3	31.9	292.9	288.3	31.2	7.5	1308	0228
AUG.	303.5	282.9	310.5	277.3	20.6	33.2	292.8	289.9	29.9	4.5	1237	0242
SEP.	299.0	279.7	305.7	274.6	19.3	31.1	291.9	286.1	29.3	7.7	1231	0249
OCT.	291.3	278.3	301.9	271.9	13.0	30.0	284.3	286.4	25.5	1.6	1242	0123
NOV.	285.5	277.7	(290)	270.7	7.8	(19.3)	281.2	285.9	15.5	0.9	1207	0117
DEC.	283.1	276.3	289.3	269.6	6.8	19.7	278.8	282.7	14.6	1.6	1300	0201
1954												
JAN.	280.0	272.1	288.3	263.6	7.9	24.7	271.8	283.8	17.0	0.3	1259	0230
FEB.	282.4	271.4	290.8	261.2	11.0	29.6	275.4	281.1	20.3	1.9	1300	0004
MAR.	289.2	274.7	299.5	(263)	14.5	(36)	274.1	281.1	26.2	1.2	1308	0141
APR.	293.4	273.6	298.9	268.5	19.8	30.4	286.6	282.6	28.5	6.2	1240	0311
YEAR	292.6	277.6	-	-	14.9	-	-	-	-	-	1248	0204

The figures for YEAR are all annual means. Bracketed figures are estimated; this had to be done occasionally when the record was defective for some reason.

G. 27181/PC/9/55/50

FIG. 1A

M.R.P. 936

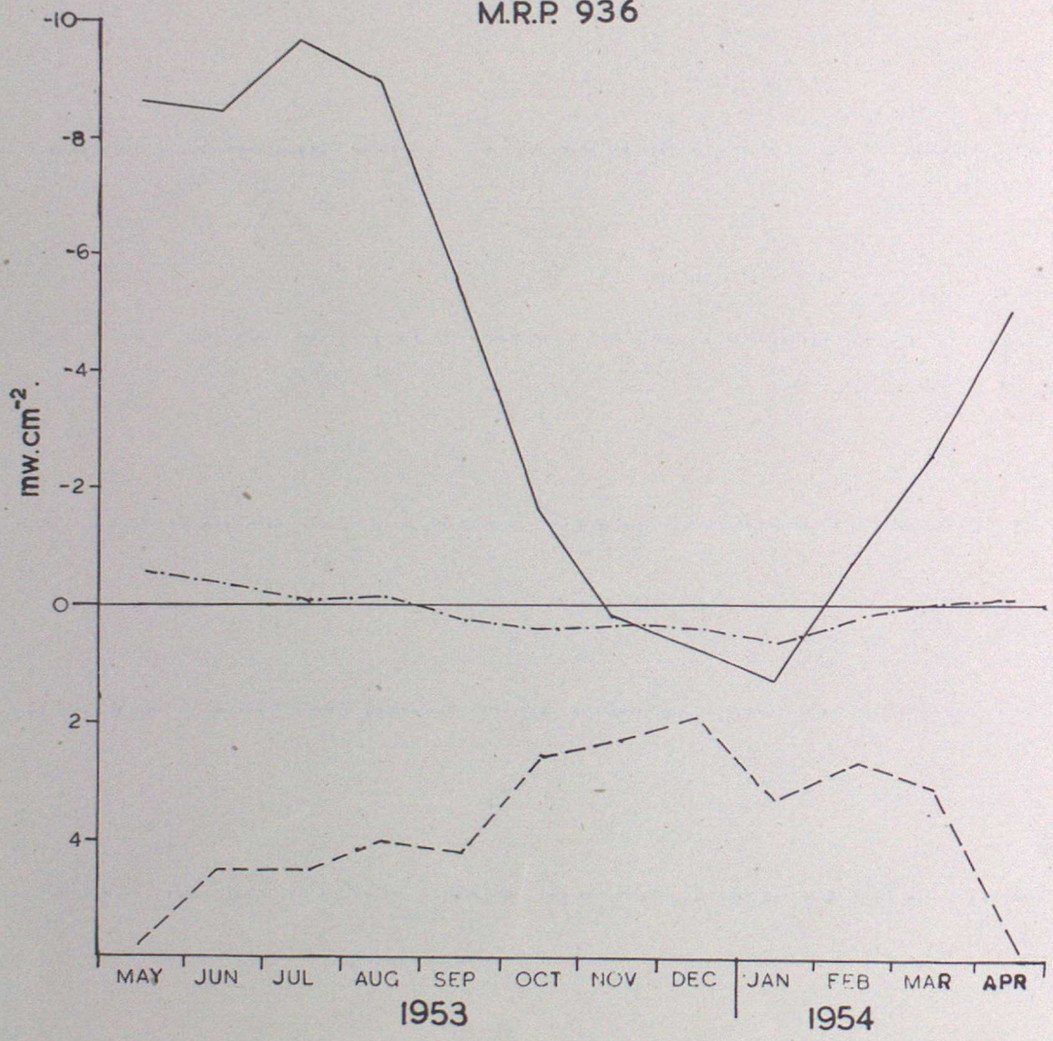

MONTHLY MEANS

FIG. 1B

MONTHLY MEANS

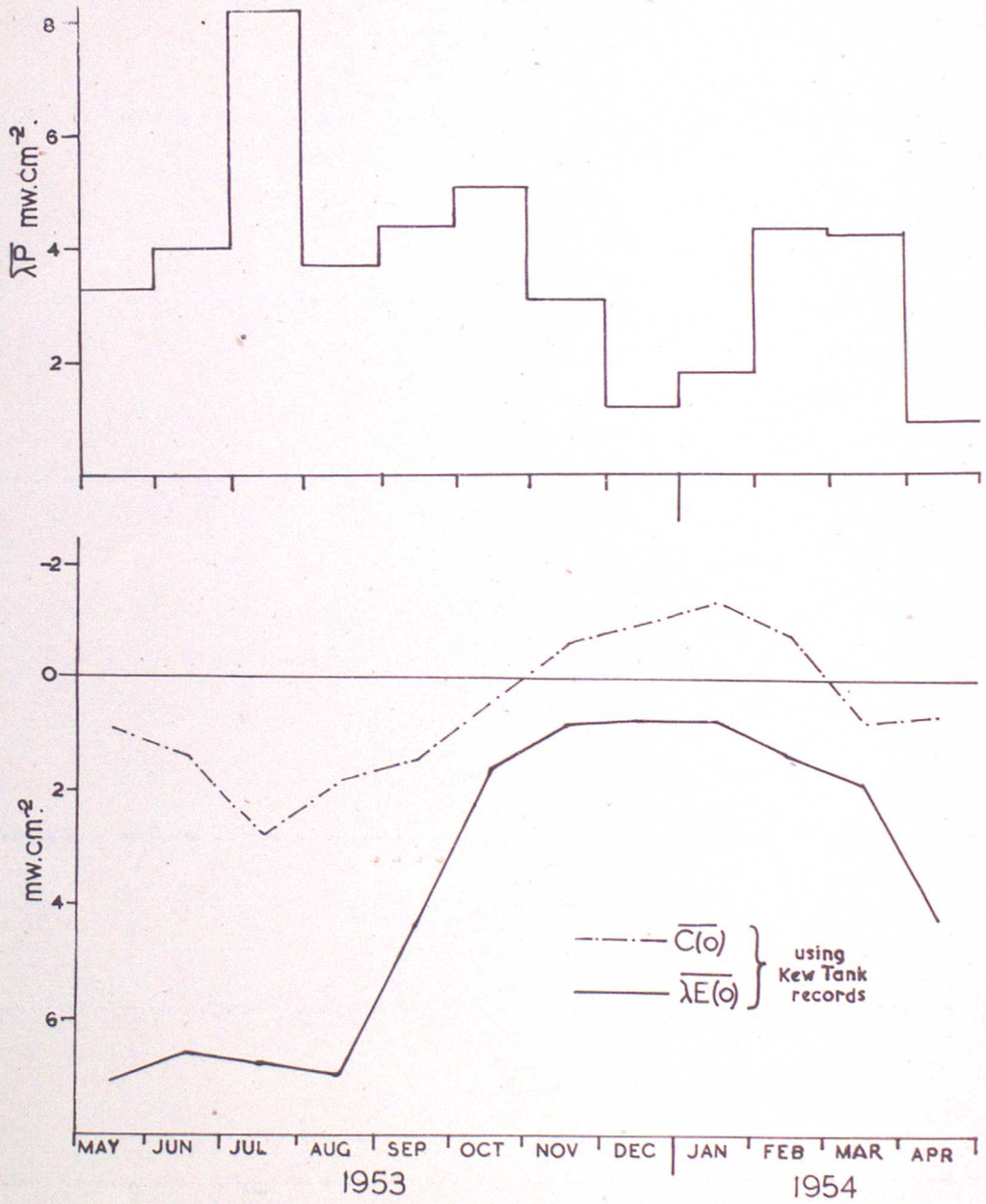

M.R.P. 936 FIG. 2

BLACK BODY CAVITY RADIATOR

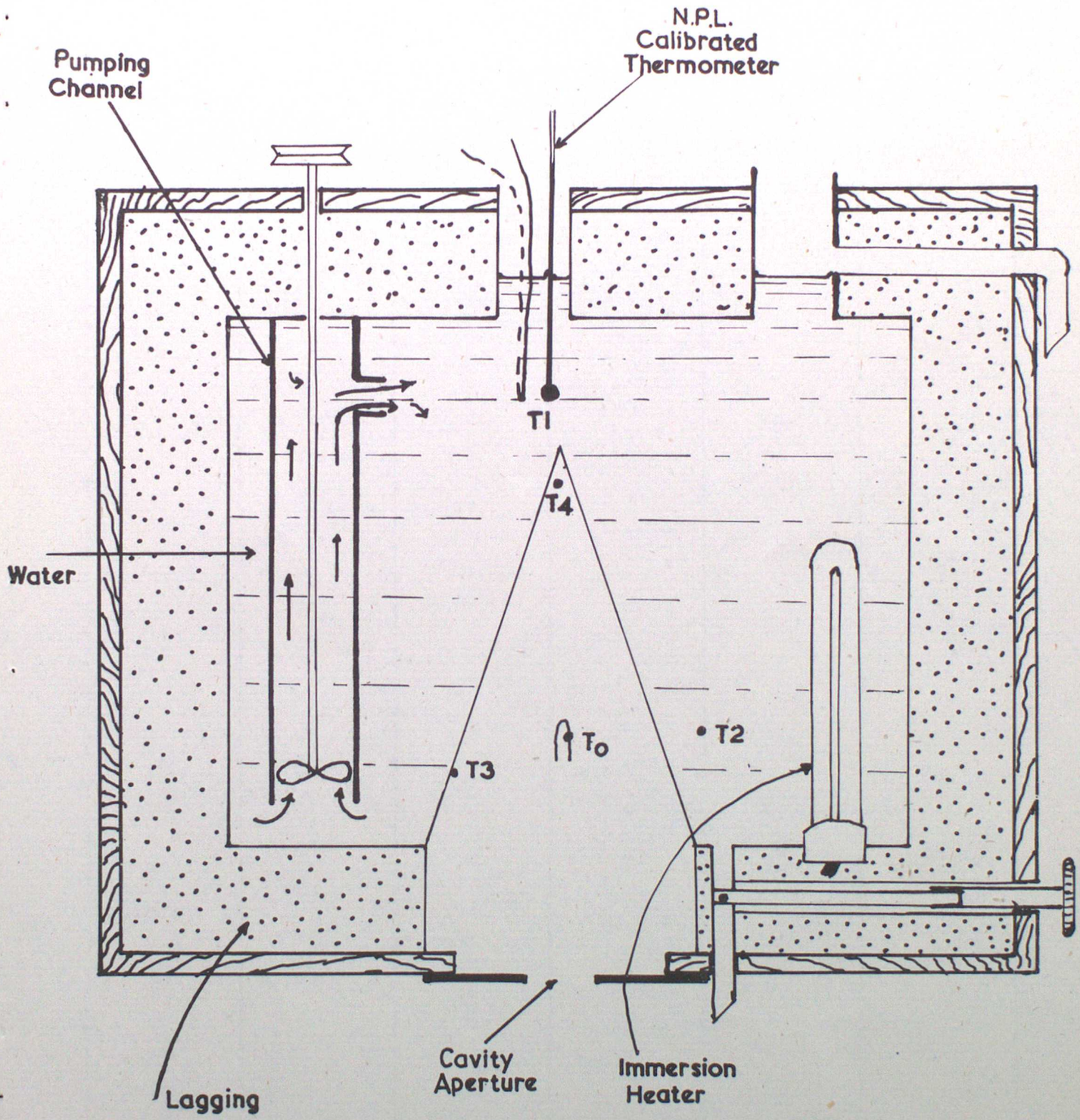

T 1,2,3,4 denote the approximate positions of fixed thermojunctions

To is a movable junction for probing the temperature field within the cavity

N.B. For a diagram of the Dines' Black Body, see MacDowall (1954).

M.R.P. 936

Chart a

4 June 1953

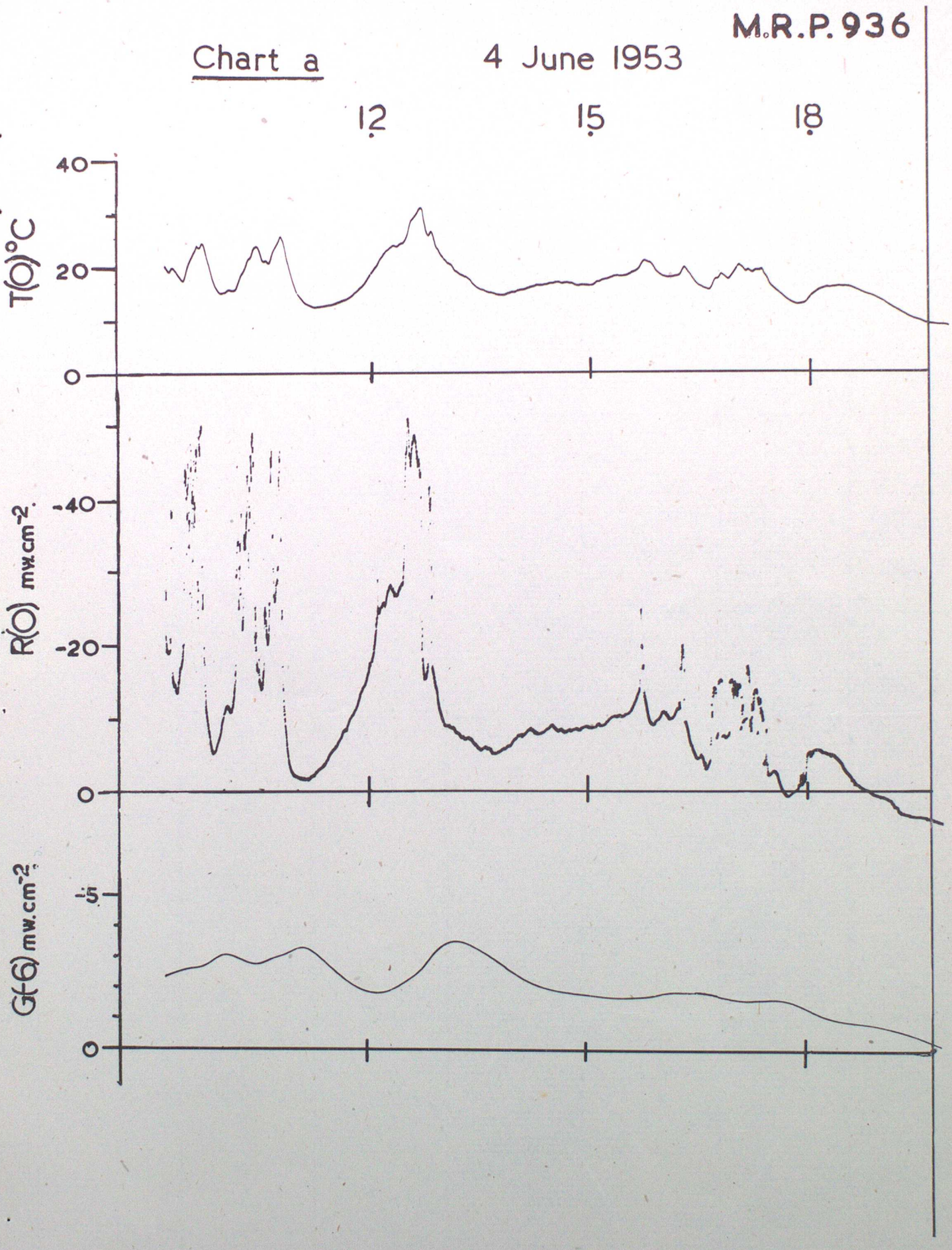

Chart b

9 June 1953

10 June 1953

12 15 18 21 24 3 6 9

T(0)°C

40 20 0

R(0) mw.cm.$^{-2}$

-40 -20 0

G(-6) mw.cm.$^{-2}$

-5 0 +2

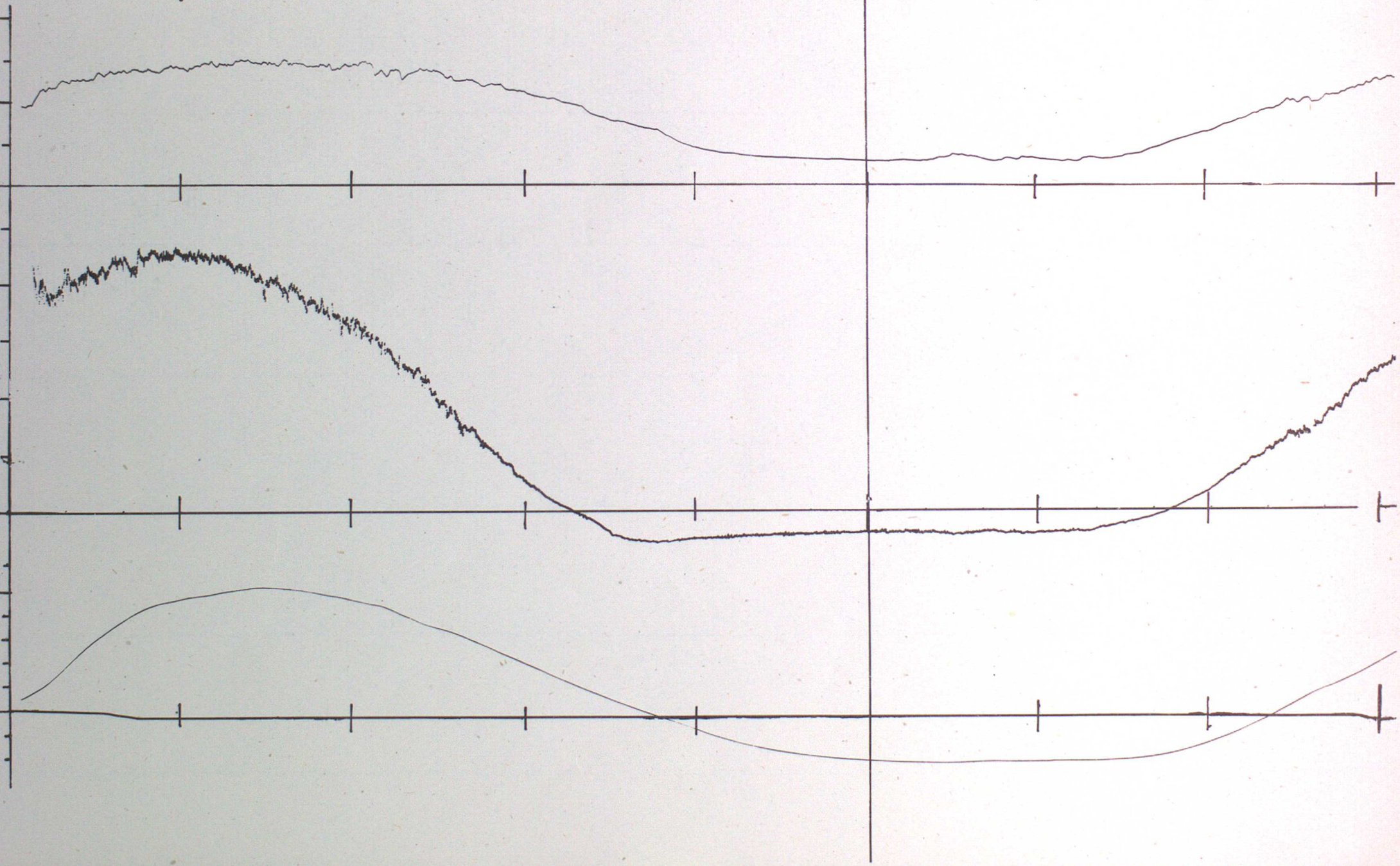

M.R.P. 936

Chart c

20 June 1953

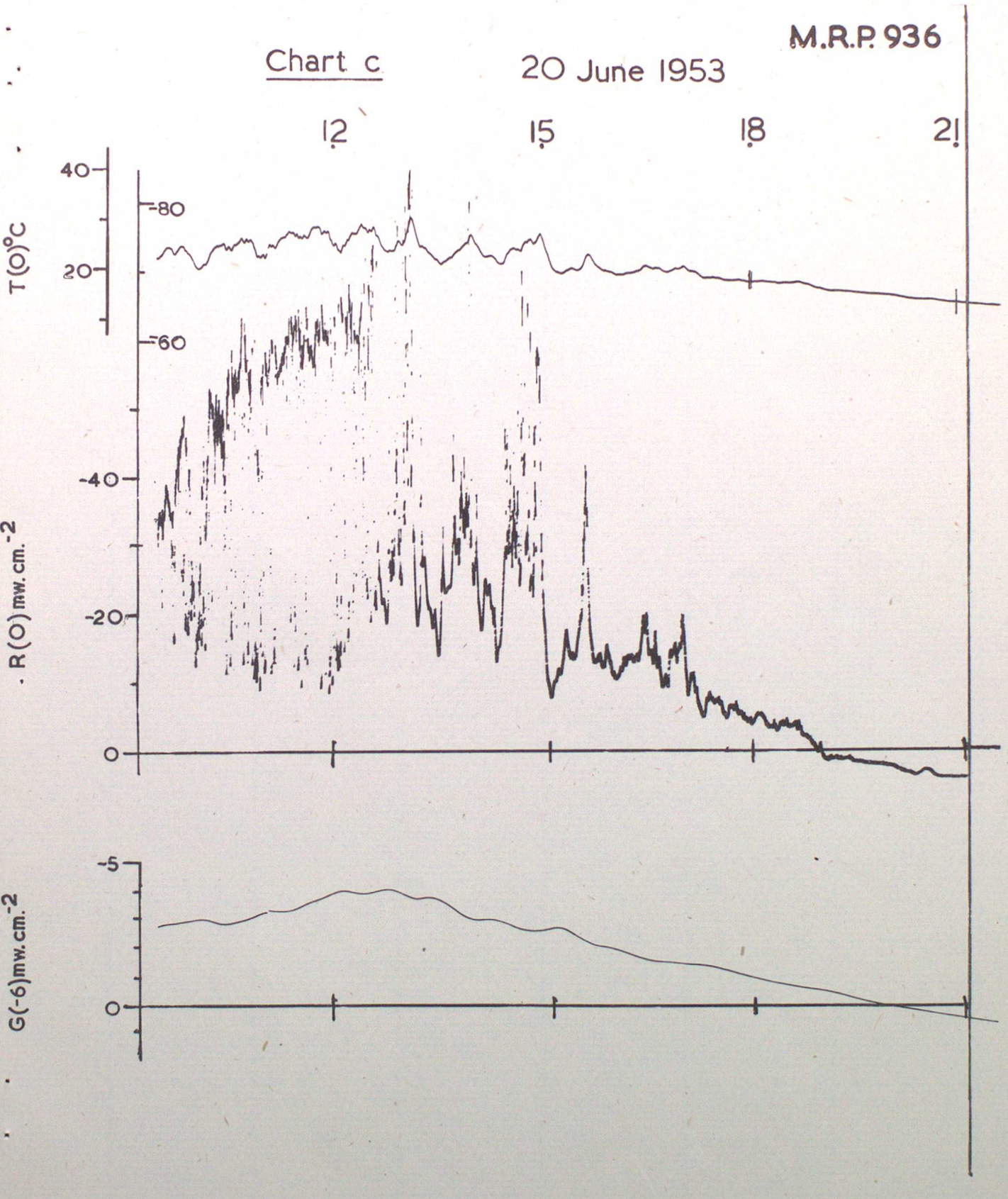

M.R.P. 936

16th | 17th

Chart d

November 1953

21 24 3

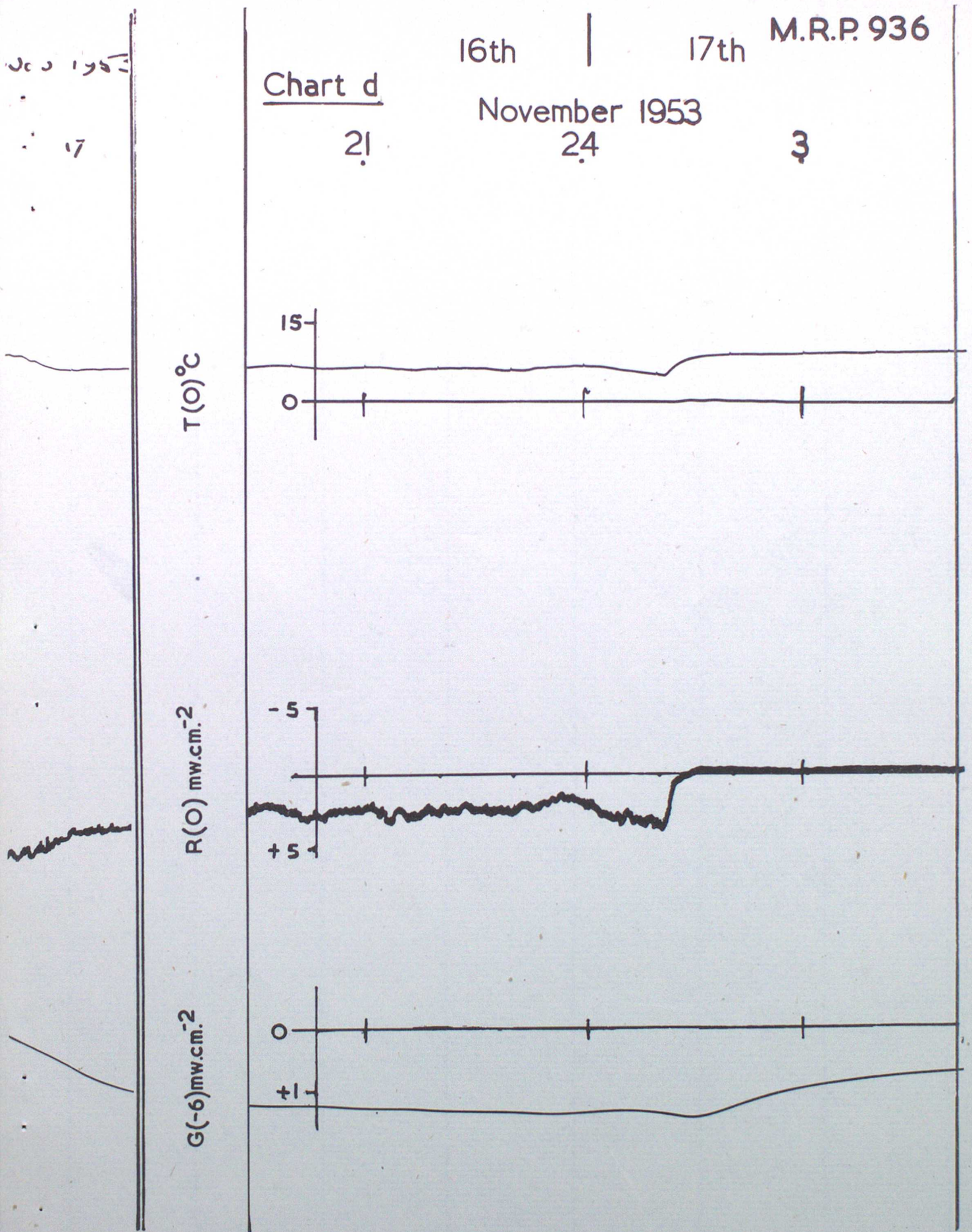

Chart e

29 November 1953

M.R.P. 936

12 15 18 21 24 30th

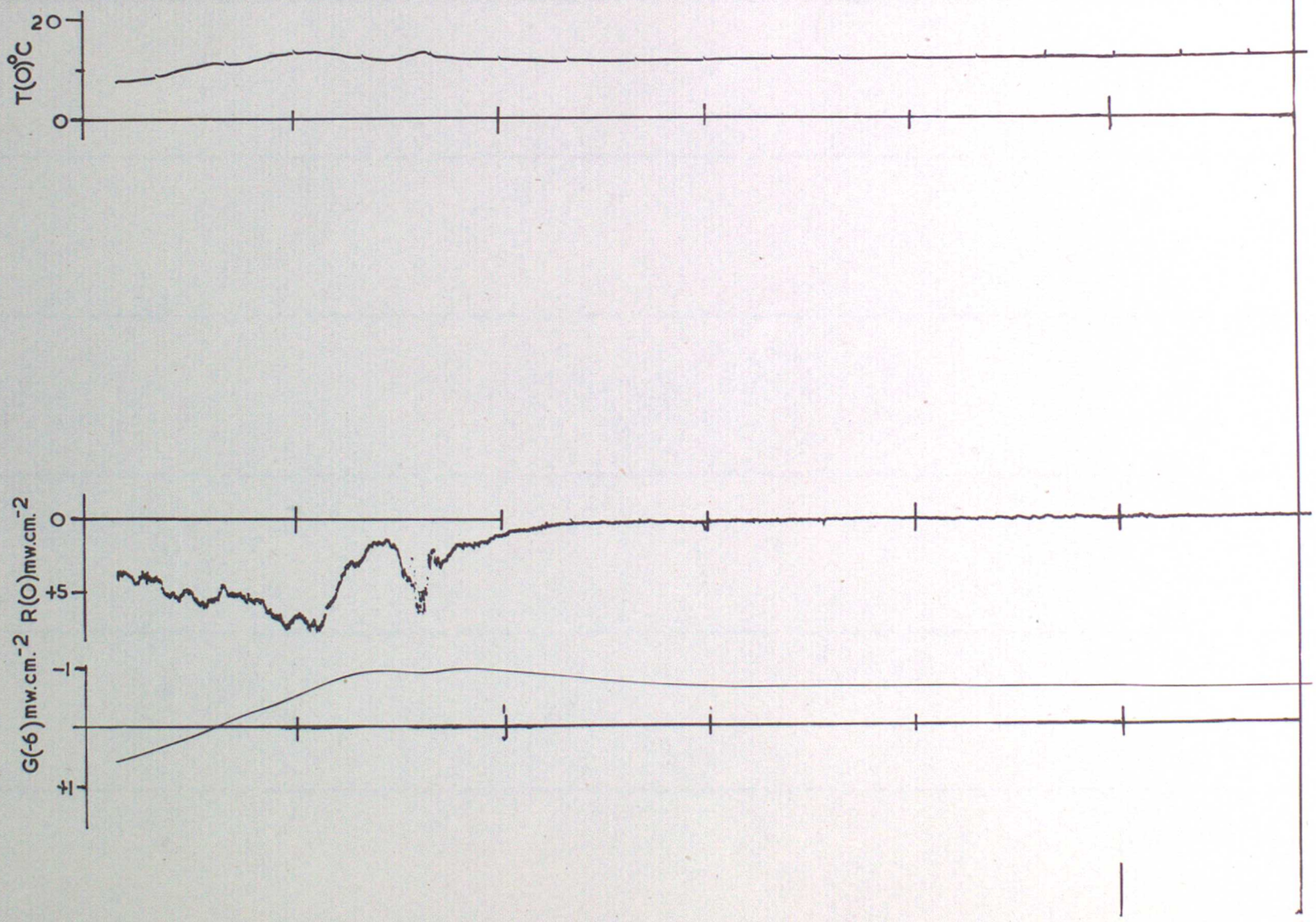

Chart f

27 January 1954 M.R.P. 936 28 January 1954

12 15 18 21 24 3 6 9

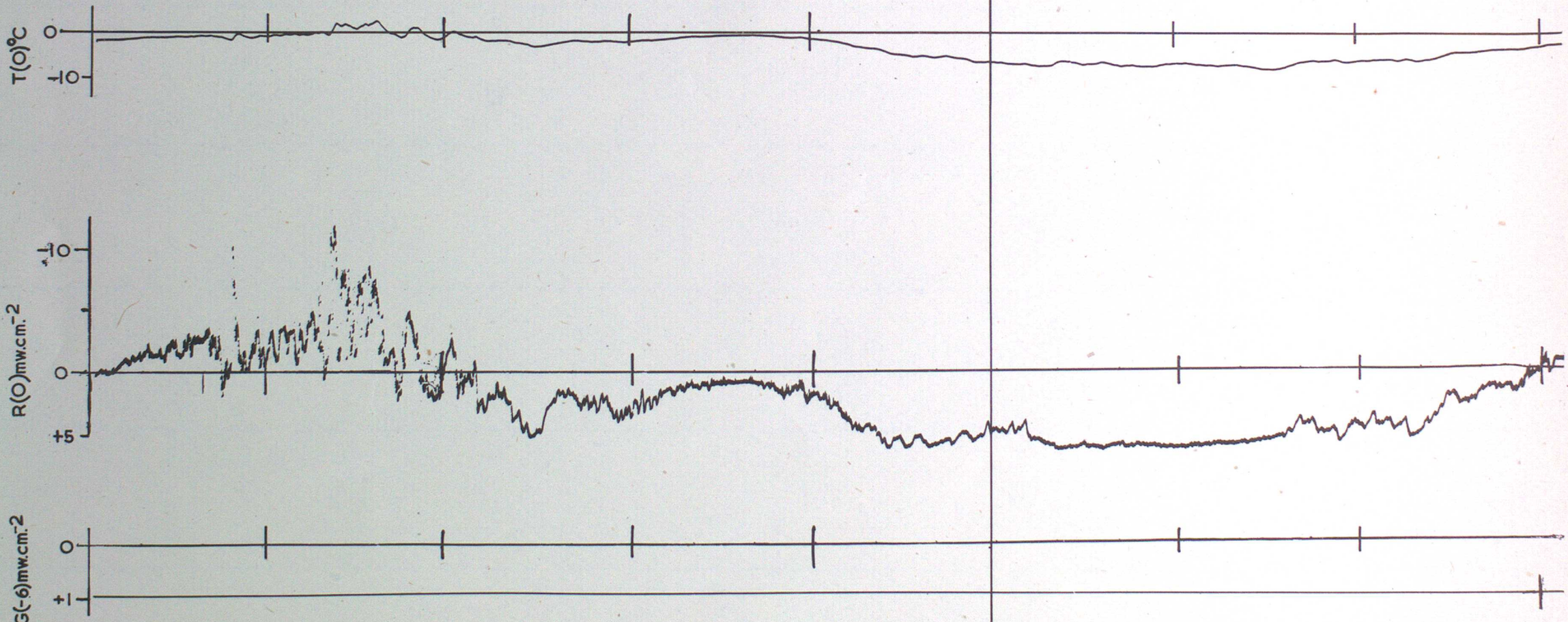

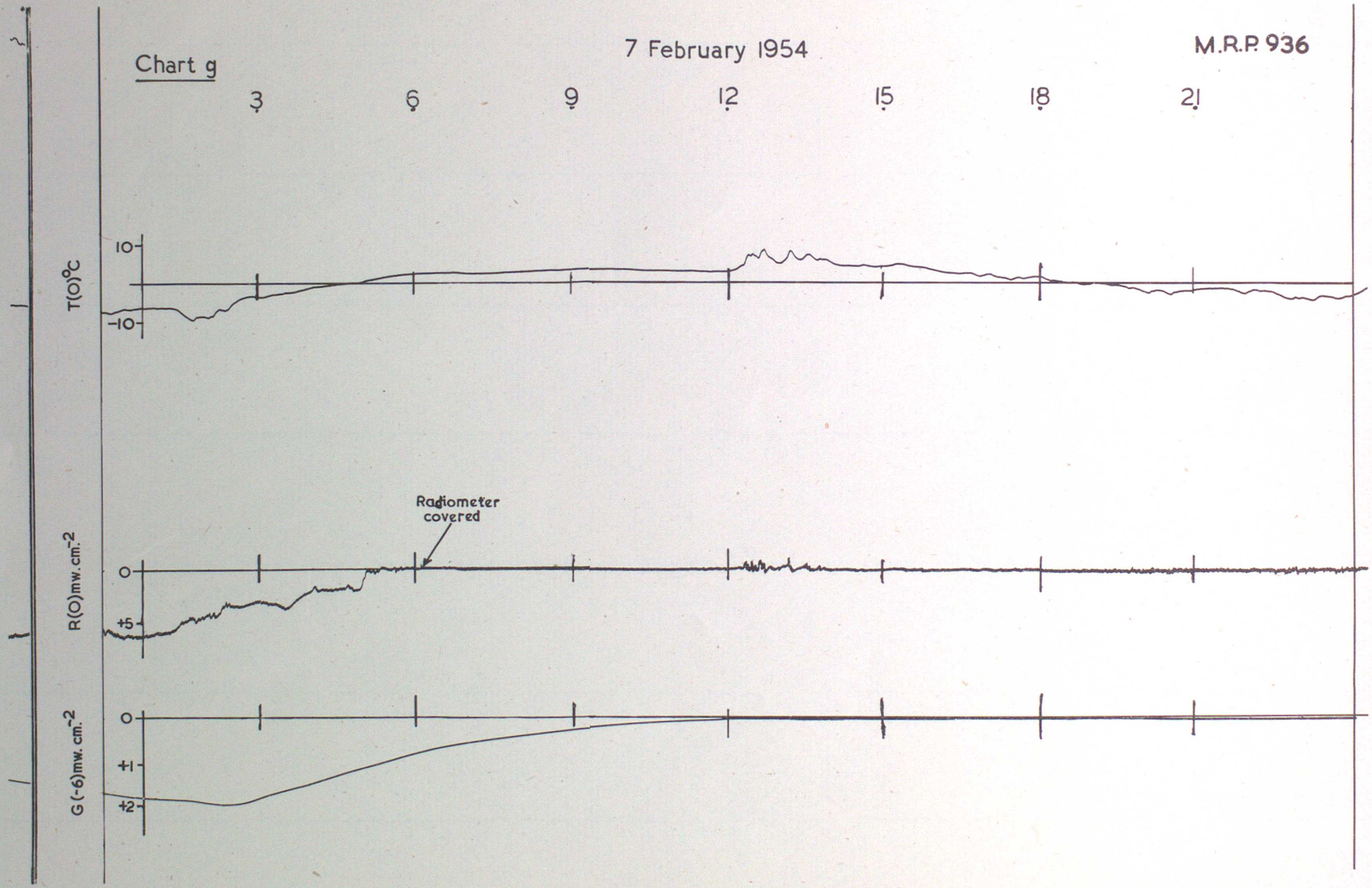
Chart g
7 February 1954
M.R.P. 936
3
6
9
12
15
18
21
T(0)°C
10
-10
R(0)mw.cm.-2
Radiometer covered
0
+5
G(-6)mw.cm.-2
0
+1
+2

M.R.P. 936

15 February 1954

Chart h

3 6 9 12 15 18

T(0)°C

10

0

R(0)mw.cm.$^{-2}$

-5

0

G(-6)mw.cm.$^{-2}$

0·5

-0·5

M.R.P. 936

Chart j

31 March 1954
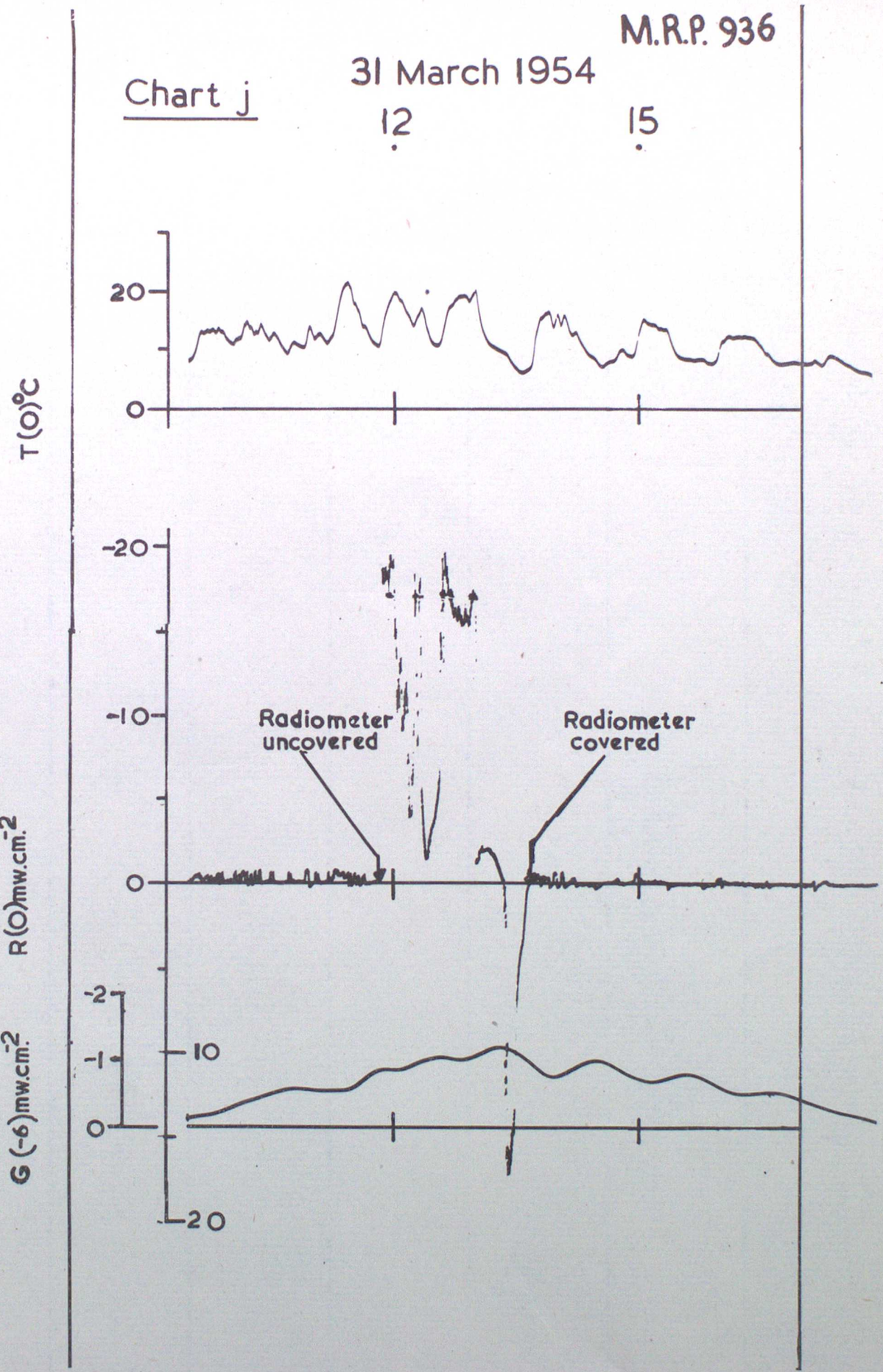
12 15